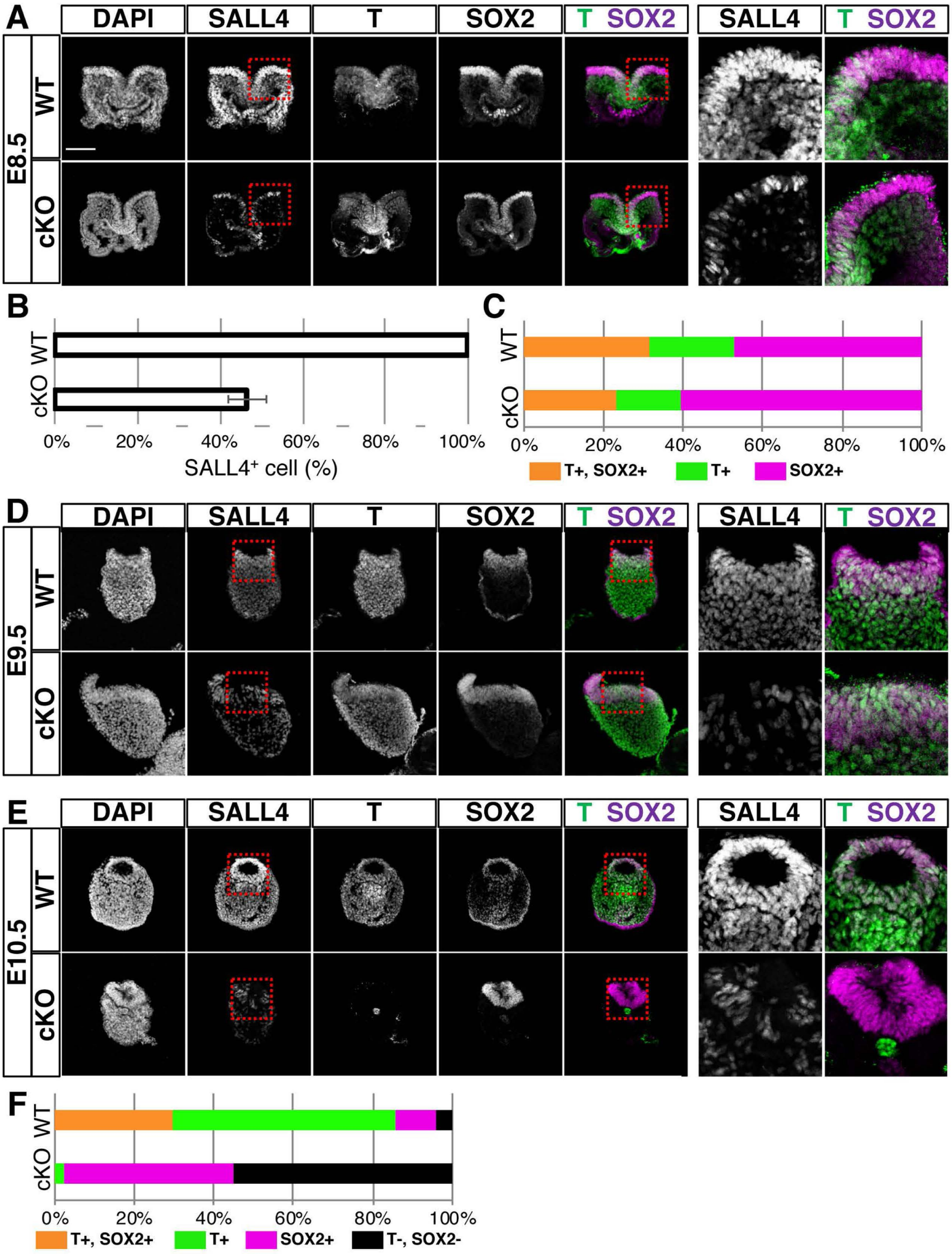
A
DAPI
SALL4
T
SOX2
T SOX2
SALL4
T SOX2
E8.5
WT
cKO
B
WT
cKO
0%
20%
40%
60%
80%
100%
SALL4⁺ cell (%)
C
WT
cKO
0%
20%
40%
60%
80%
100%
T+, SOX2+
T+
SOX2+
D
DAPI
SALL4
T
SOX2
T SOX2
SALL4
T SOX2
E9.5
WT
cKO
E
DAPI
SALL4
T
SOX2
T SOX2
SALL4
T SOX2
E10.5
WT
cKO
F
WT
cKO
0%
20%
40%
60%
80%
100%
T+, SOX2+
T+
SOX2+
T-, SOX2-

Fig. S1 Immunofluorescence of WT and *Sall4* cKO embryos

(A) Confocal images of caudal part of E8.5 embryos stained on sections.

(B, C) Quantitation of SALL4+ cells (B) and cells with different combinations of T and SOX2 (C) in whole mount-stained embryos. n=5 for WT and *Sall4* cKO

(D) Confocal images of caudal part of E9.5 embryos stained on sections.

(E) Confocal images of caudal part of E10.5 embryos stained on sections.

Two right columns in A, D, E show closeup images of the boxed areas. Single channel images are shown in black/white. Merged images are shown with green (T) and magenta (SOX2).

(F) Quantitation of cells with different combinations of T and SOX2 in sections in the posterior. n=5 for WT and n=4 for *Sall4* cKO

Scale bar = 100 μm.

Fig. S2

Fig. S2 Heat map of genes with neural differentiation GO terms between WT and *Sall4* cKO embryos

Heat map of genes with neural differentiation GO terms in WT vs *Sall4* mutants.

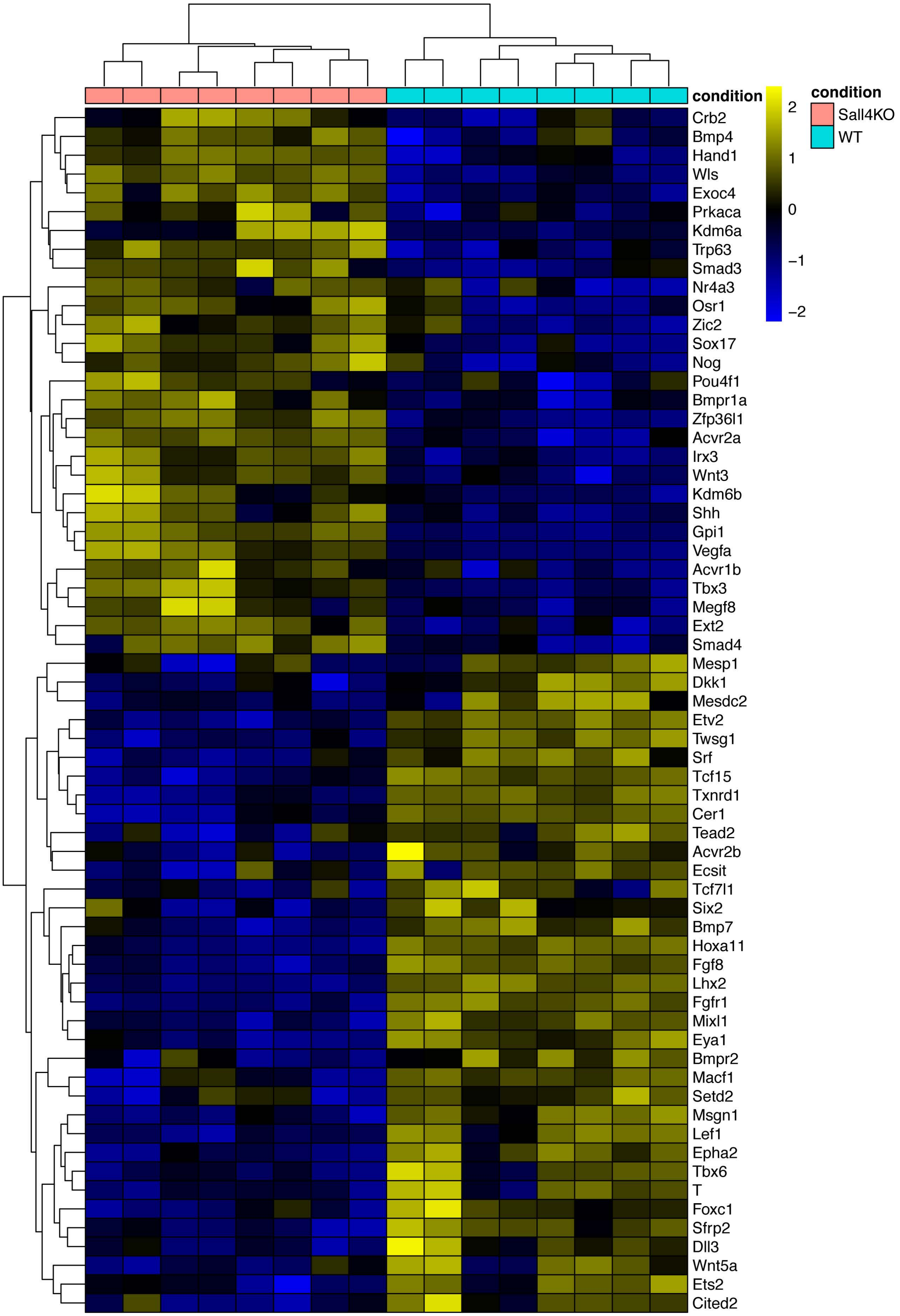
condition
Crb2
Bmp4
Hand1
Wls
Exoc4
Prkaca
Kdm6a
Trp63
Smad3
Nr4a3
Osr1
Zic2
Sox17
Nog
Pou4f1
Bmpr1a
Zfp36l1
Acvr2a
Irx3
Wnt3
Kdm6b
Shh
Gpi1
Vegfa
Acvr1b
Tbx3
Megf8
Ext2
Smad4
Mesp1
Dkk1
Mesdc2
Etv2
Twsg1
Srf
Tcf15
Txnrd1
Cer1
Tead2
Acvr2b
Ecsit
Tcf7l1
Six2
Bmp7
Hoxa11
Fgf8
Lhx2
Fgfr1
Mixl1
Eya1
Bmpr2
Macf1
Setd2
Msgn1
Lef1
Epha2
Tbx6
T
Foxc1
Sfrp2
Dll3
Wnt5a
Ets2
Cited2
2
1
0
−1
−2
condition
Sall4KO
WT

Fig. S3 Heat map of genes with mesoderm development GO terms between WT and *Sall4* cKO embryos

Heat map of genes with mesoderm development GO terms in WT vs *Sall4* mutants.

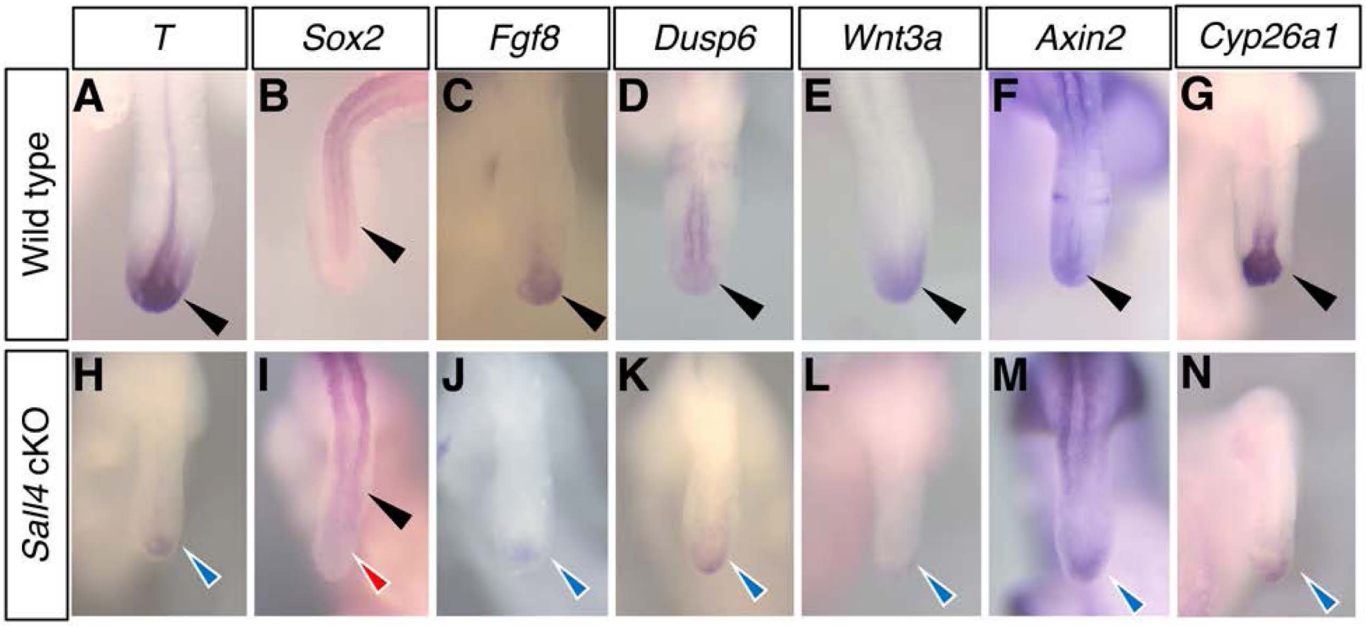

Fig. S4 Expression pattern of genes at E10.5 in WT and *Sall4* cKO embryos

Whole mount in situ hybridization of indicated genes in WT (A-G) and *Sall4* cKO (H-N) at E10.5. Black arrowheads point to normal expression in the posterior tip of the body in WT embryos (A-G) and *Sox2* expression in the *Sall4* cKO embryo (I). Blue arrowheads point to reduced expression in *Sall4* cKO embryos (H, J-N). Red arrowhead in I points to upregulated *Sox2* expression in the *Sall4* cKO embryo.

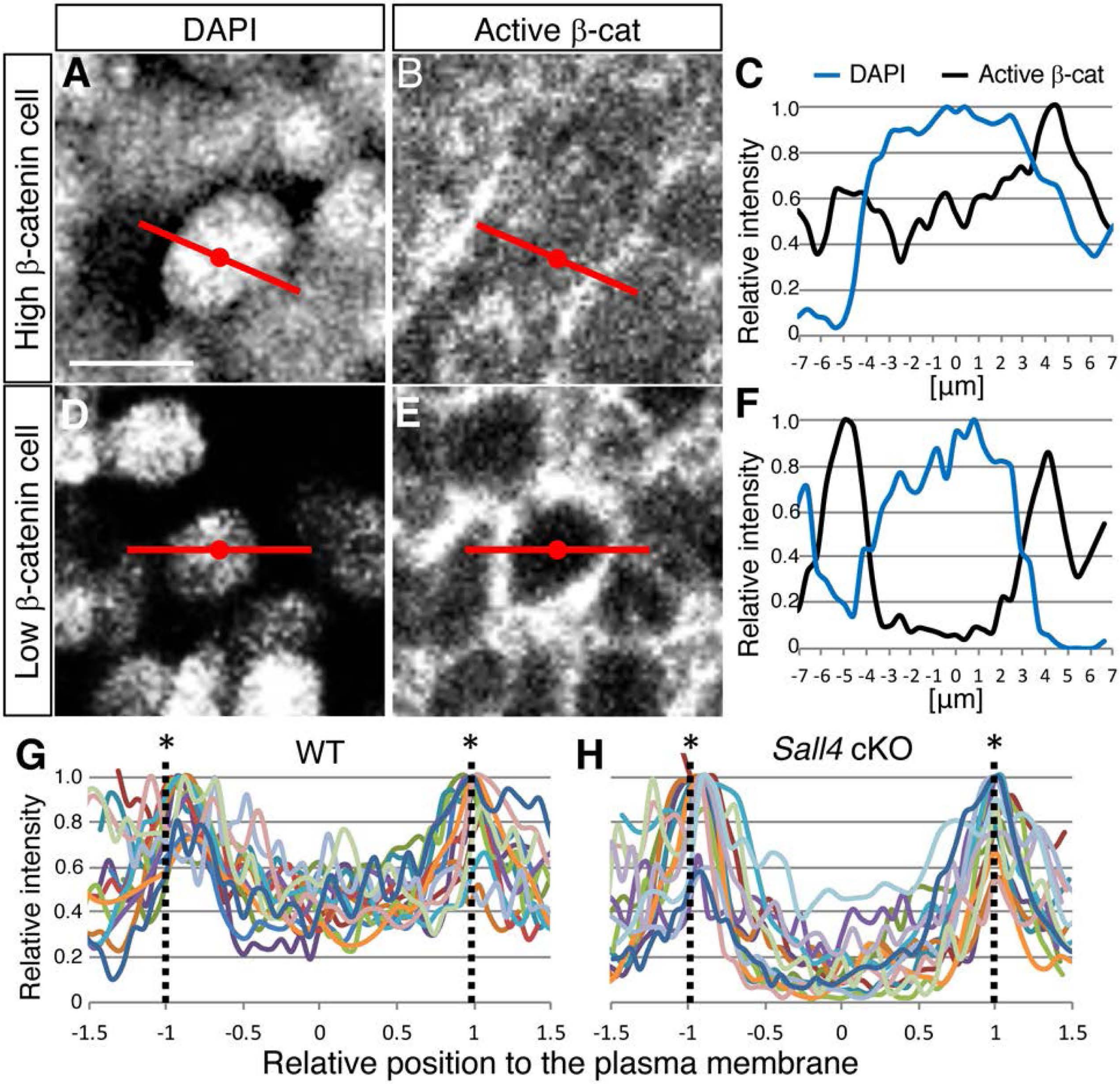
DAPI
Active β-cat
High β-catenin cell
Low β-catenin cell
A
B
C
D
E
F
G
H
DAPI
Active β-cat
Relative intensity
0
0.2
0.4
0.6
0.8
1.0
-7 -6 -5 -4 -3 -2 -1 0 1 2 3 4 5 6 7
[µm]
*
WT
Sall4 cKO
-1.5
-1
-0.5
0
0.5
1
1.5
Relative position to the plasma membrane

Fig. S5 Reduced levels of nuclear ß-catenin in *Sall4* cKO embryos

(A-F) Typical single plane images of cells with high nuclear active ß-catenin (A-C) and cells with low nuclear active ß-catenin (D-F). Red dots positions at the center of the nucleus. Red lines indicate the line along which ß-catenin signal intensity shown in C and F was measured. Scale bar = 10 µm. In C and F, the highest ß-catenin signal intensity at the plasma membrane is set as 1.0, and the highest nuclear DAPI signal in the nucleus is set as 1.0. Relative intensities of ß-catenin and DAPI signals to the highest signal are shown. Scale bar = 10 µm.

(G, H) Relative intensities of ß-catenin signals of 15 cells randomly selected from the posterior of WT (G) and *Sall4* cKO (H) embryos. Because each cell size is different, the positions of plasma membrane of each cell are normalized to be -1 and 1 along the x axis, and the highest ß-catenin signal intensity of each cell is normalized to be 1.0 along the y axis. WT cells exhibit higher levels of nuclear ß-catenin than *Sall4* cKO cells.

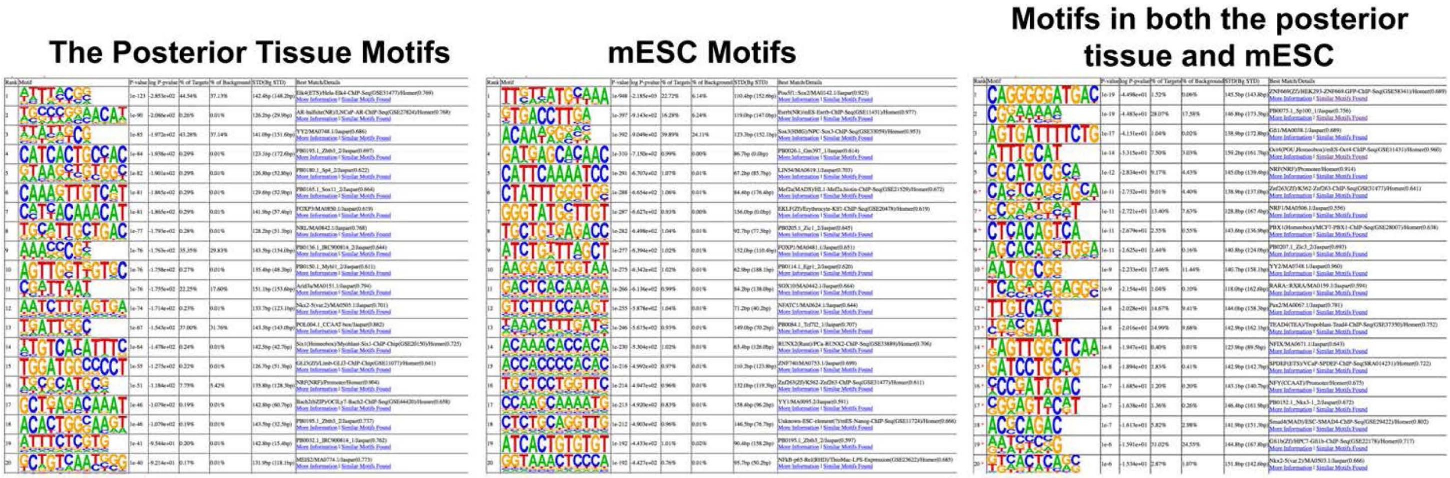

Fig. S6 Transcription factor motifs in the SALL4 enriched sequences

Top 20 de-novo motifs found in SALL4-enriched sequences in the posterior tissue, mESCs, and peaks in both cell/tissue types by Homer analysis.

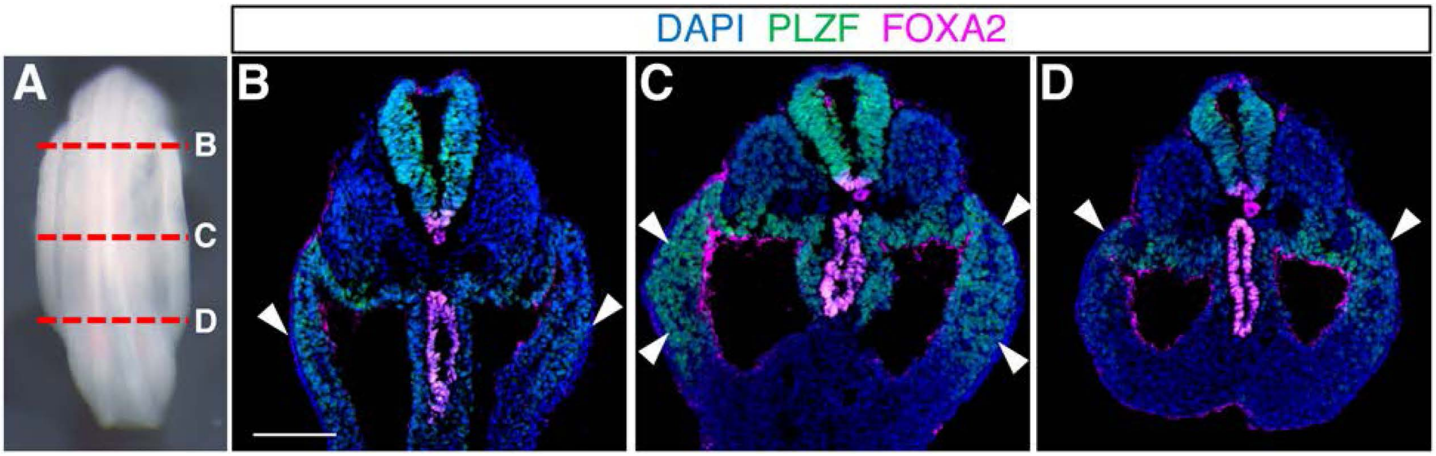

Fig. S7 Examples of PLZF immunofluorescence of E9.75 embryos at the hindlimb level

(A) Dorsal view of an E9.75 embryo at the hindlimb level.

(B-D) Immunofluorescence of PLZF (green) and FOXA2 (magenta) at the anterior (B), middle (C) and posterior (D) hindlimb levels. Arrowheads point to PLZF expression in the hindlimb mesenchyme. Scale bar = 100 µm.

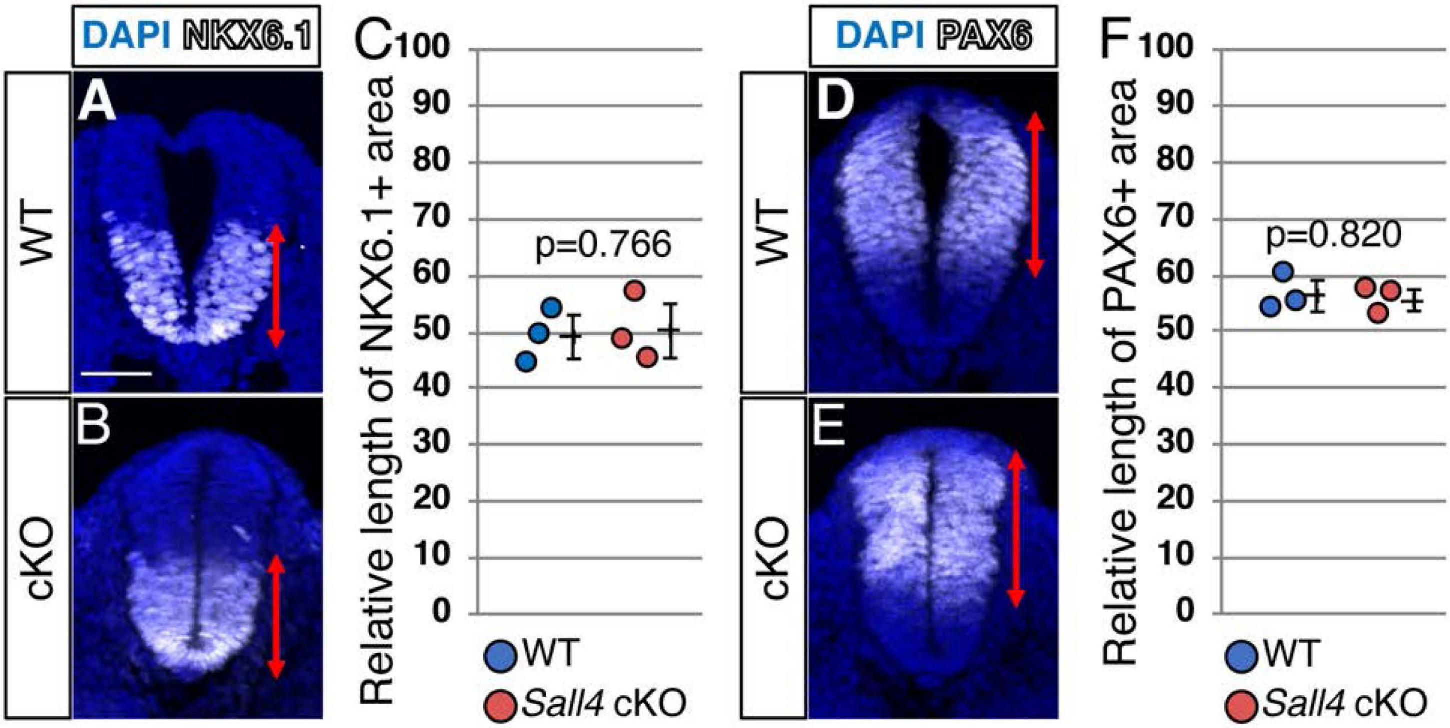

Fig. S8 NKX6.1 and PAX6 expression in the neural tube

(A, B) Immunofluorescence of NKX6.1 in WT (A) and *Sall4* cKO (B) embryos at the posterior hindlimb level at E10.25 (33/34 somite stage). Red double arrowhead line shows the length of the NKX6.1 expressing domain along the dorsal-ventral axis of the neural tube.

(C) Quantification of the length of the NKX6.1 expressing domain along the dorsal-ventral axis of the neural tube. P values by unpaired *t-test* are shown within the panel. n=3 for both WT and *Sall4* cKO.

(D, E) Immunofluorescence of PAX6 in WT (D) and *Sall4* cKO (E) embryos at the posterior hindlimb level at E10.25 (33/34 somite stage). Red double arrowhead line shows the length of the PAX6 expressing domain along the dorsal-ventral axis of the neural tube.

(F) Quantification of the length of the NKX6.1 expressing domain along the dorsal-ventral axis of the neural tube. P values by unpaired t-test are shown within the panel. n=3 for both WT and *Sall4* cKO.

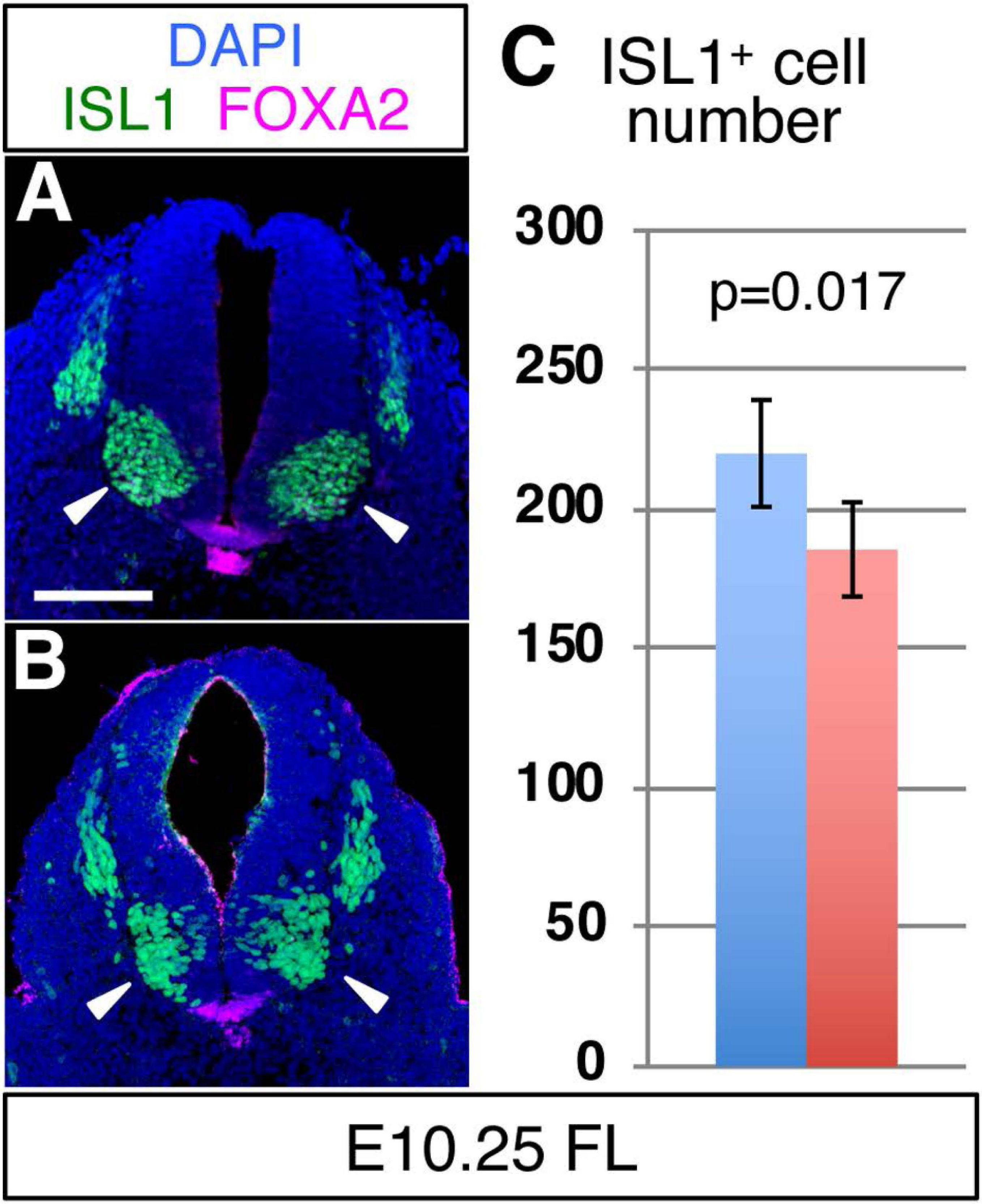
DAPI
ISL1 FOXA2
A
B
C
ISL1+ cell number
300
250
200
150
100
50
0
p=0.017
E10.25 FL

Fig. S9 Immunofluorescence analysis of neural tube in WT and *Sall4* cKO embryos at the forelimb bud level

(A, B) Immunofluorescence of ISL1 (green) and FOXA2 (magenta) in WT (A) and *Sall4* cKO (B) embryos at the forelimb level at E10.25. White arrowheads point to ISL1 positive cells. Scale bar = 100 µm.

(C) Quantification of ISL1 positive cells at the forelimb level at E10.25. p value is shown within the panel. n=5 for both WT and *Sall4* cKO.

Table S1. Statistical examination of differences of cell type populations between WT and *Sall4* cKO posterior tissue

Tested hypothesis: T+/SOX2+ ratio is different between WT and *Sall4* cKO

Stage	P value
E8.5	< 2.2e-16
E9.5	6.139e-15
E10.5	< 2.2e-16

Two proportion Z test was used to examine differences.

At E8.5 and E9.5, whole mount stained embryos were analyzed. At E8.5, n=5 (WT and *Sall4* cKO). At E9.5, n=4 (WT) and n=3 (*Sall4* cKO).
At E10.5, n=5 (WT) and n=4 (*Sall4* cKO). A section that includes the chord-neural hinge region was analyzed from each embryo.

Table S2: SALL4-enrichment near the genes known to participate in NMP renewal

SALL4-enrichment near *Sox2*, *T*, *Cdx2*, *Fgf8*, *Wnt3a*, *Cyp26a1* and genes belonging to FGF signaling (GO:0008543) and WNT signaling (GO:0016055) are shown.

Click here to download Table S2

Table S3. List of antibodies and their dilution conditions for immunofluorescence

Primary antibodies

Active-β-catenin: Millipore/Upstate, #05-665, #2377065, mouse, 1/250

active caspase 3: BD Bioscience, 559565, rabbit, 1/200

Brachyury: Santa Cruz Biotechnology, sc-17743, goat, 1/100

DBX1: Vue TY*, et al.* (2007), rabbit, 1/100

FOXA2: Santa Cruz Biotechnology, sc-6554, goat, 1/200

ISL1: Developmental Studies Hybridoma Bank, 39.4D5-c, mouse, 4 µg/ml

LEF1: Cell Signaling Technology, 2230P, C12AS, rabbit, 1/100

NKX2.2: Abcam, ab191077, rabbit, 1/1000

NKX6.1: R&D Systems, AF5858, goat, 15 µg/ml

OLIG2: R&D Systems, AF2418, goat, 1/200

phospho Histone H3: Millipore, 06-570, rabbit, 1/100

PAX6: BD Bioscience, 561462, mouse, 1/500

PLZF: Santa Cruz Biotechnology, sc-22839, rabbit, 1/100

SALL4: Santa Cruz Biotechnology, sc-101147 (EE30), mouse, 1/300

SHH: R&D Systems, AF445, goat, 1/20

SOX1: R&D Systems, AF3361, goat, 1/100

SOX2: Millipore, AB5603, rabbit, 1/500

SOX2: R&D, MAB2018, mouse, 1/400

Secondary antibodies

Donkey anti-Mouse IgG Alexa 488, Invitrogen, A-21202, 1/500

Donkey anti-Rabbit IgG Alexa 647, Invitrogen, A-31573, 1/500

Donkey anti-Goat IgG Alexa 488, Invitrogen, A-11055, 1/500

Donkey anti-Goat IgG Alexa 594, Invitrogen, A-11058, 1/500

Goat anti-Mouse IgG Alexa 488, Invitrogen, A-11001, 1/500

Goat anti mouse IgG Alexa 594 Invitrogen, A-11005, 1/500

Goat anti-Rabbit IgG Alexa 488, Invitrogen, A-11008, 1/500

Goat anti-Rabbit IgG Alexa 594, Invitrogen, A-11012, 1/500

Goat anti-rabbit IgG Alexa 555, Invitrogen, A-21428, 1/500

Vue TY*, et al.* (2007) Characterization of progenitor domains in the developing mouse thalamus. *J Comp Neurol* 505(1):73-91.